Magnetic Ligand Fishing Using Immobilized Cyclooxygenase-2 for Identification and Screening of Anticoronary Heart Disease Ligands From *Choerospondias axillaris*

Miaomiao Chi[1], Hongsen Wang[2], Zhankuan Yan[2], Lei Cao[1], Xun Gao[1,3,4]* and Kunming Qin[1]*

[1] Jiangsu Key Laboratory of Marine Pharmaceutical Compound Screening, Jiangsu Ocean University, Lianyungang, China, [2] Jiangsu Original Drug Research and Development Co., Ltd., Lianyungang, China, [3] Jiangsu Institute of Marine Resources Development, Jiangsu Ocean University, Lianyungang, China, [4] Co-Innovation Center of Jiangsu Marine Bio-industry Technology, Jiangsu Ocean University, Lianyungang, China

Inhibition of cyclooxygenase-2 (COX-2) activity is an effective way for treatment of coronary heart disease. And as an important source of COX-2 inhibitors, bioactive compounds of *Choerospondias axillaris* and pharmacological mechanisms remained lacking in prospective researches. Therefore, for the purpose of accelerating the discovery of natural products targeting designed inhibitors, the COX-2 microreactor composed of functionalized microspheres and magnetic ligand fishing was developed and applied in *Choerospondias axillaris*, and the physicochemical properties of the COX-2 functionalized microspheres were characterized using Fourier transform infrared spectroscopy (FT-IR), vibrating sample magnetometer (VSM), scanning electron microscopy (SEM), and transmission electron microscopy (TEM). Furthermore, the bioactive compounds singled out from ethanol decoction without prepurification were dissociated and identified by ultraperformance liquid chromatography plus Q-Exactive Orbitrap tandem mass spectrometry (UPLC-Q-Exactive Orbitrap-MS/MS). Consequently, 21 bioactive compounds consisting of 6 organic acids, 8 flavonoids, and 7 others were separated and characterized from *Choerospondias axillaris*, which were reported to participate in the COX-2 inhibitory pathway to varying degrees. Therefore, this method could provide a prospective solution for the extraction and identification of active pharmaceutical ingredients and the rapid screening of some enzyme inhibitors in the complex mixtures.

Keywords: cyclooxygenase-2, magnetic ligand fishing, *Choerospondias axillaris*, UPLC-Q-Exactive Orbitrap-MS/MS, traditional Chinese medicine

INTRODUCTION

In most countries, the prevalence of the cardiovascular disease is still on the rise. *Choerospondias axillaris* has been used in China to treat the coronary heart disease as early as the eighth century (1). Modern pharmacological researches also showed that *Choerospondias axillaris* was used to treat cardiovascular diseases because of its antiarrhythmia and antimyocardial ischemia effects (2, 3).

However, due to its complex chemical composition, there are few studies on the specific functional components representing the specific pharmacological activities of *Choerospondias axillaris* and their corresponding targets (4).

The results of network pharmacology and pharmacokinetic studies suggest that the flavonoids and organic acids may be the material basis for the prevention and treatment of coronary heart disease in *Choerospondias axillaris* (5). Flavonoids may mediate the cGMP-PKG signaling pathway, and organic acids such as gallic acid, protocatechuic acid, and chlorogenic acid may mediate the Wnt signaling pathway to jointly play the role of preventing and treating coronary heart disease. Moreover, the prevention and treatment of coronary heart disease may be related to related biological processes such as stress response, immune-inflammatory response, signal transduction, and atherosclerotic plaque instability by *Choerospondias axillaris*. COX-2 was reported to be a key enzyme that participated in platelet aggregation, and regulate the resistance of peripheral blood vessels and the distribution of renal blood flow (6–8). Therefore, it is of great importance that started with COX-2 to study the active pharmaceutical compounds and their mechanism of action from *Choerospondias axillaris*.

Screening methods for active compounds of COX-2 inhibitors in Chinese medicine mainly include classic separation and activity testing methods (9), chip technology (10), high-throughput screening methods (11), and virtual ligand screening methods using structural information (12); however, the above methods have disadvantages such as large workload, long cycle, and easy loss of active compounds. Since drugs in the body exert their pharmacological effects by interacting with a variety of related biological target molecules, such as enzymes, receptors, DNA, and RNA, during the development of the disease, the ligand capture technology has become an efficient screening method guided by biological activity and based on affinity screening, which can not only quickly and target the active ingredients of traditional Chinese medicines, but also help to explain the mechanism of action of traditional Chinese medicines at the molecular level, thereby providing new methods and ideas for the treatment of diseases.

Magnetic ligand fishing is a combination of specific ligand affinity and magnetic separation, which has been proven to be a convenient and effective tool for extracting biologically active ingredients in extracts of plant. Though modern analytical techniques such as HPLC, LC-MS, and SPE-HPLC-NMR can achieve rapid identification and full structural characterization of constituents in complex matrixes, it was difficult that provide related information about biologically active ingredients. Magnetic ligand fishing detects active ingredients by binding affinity directly from the crude extract without the process of prepurification (13). However, when some ingredients produced false-positive results in ligand fishing due to the non-specific binding of immobilized enzymes, the risk can be effectively reduced by docking the protein structure of COX-2. When combined with proteins, graphene oxide (GO) can maintain the ligand structure and physiological activity because of the hydrophobic and hydrogen bonding with proteins, which indicated that GO can be used in magnetic ligand fishing.

Magnetic ligand fishing has been applied to isolate the ligands of human serum albumin (14), α-amylase (15), α-glucosides (16), cyclooxygenase-1 (COX-1) (17), and acetylcholine ester (18).

With the continued need for fast and sensitive methods for the identification of COX-2 inhibitory compounds of natural origin, we established the first application of *Choerospondias axillaris* by a combination of GO-based magnetic ligand fishing and UPLC-Q-Exactive Orbitrap-MS/MS. Because of the binding affinity of the COX-2 ligand, the use of the newly magnetic nanomaterials in ligand fishing is not limited to the crude extracts of *Choerospondias axillaris*, and the materials showed excellent specificity, good precision, and high reusability in the experiment.

MATERIALS AND METHODS

Chemicals and Reagents

Graphene oxide was purchased from the Nanjing Jicang Nano Technology Co., Ltd (Nanjing, China). Human recombinant COX-2 and methanol (HPLC grade) were supplied by Sigma (St. Louis, MO, USA). 3-aminopropyltriethoxysilane (APTES), tetraethyl orthosilicate (TEOS), glutaraldehyde (25% (w/v) aqueous solution), acetic acid (HPLC grade), ethanol, acetonitrile, $FeCl_3 \cdot 6H_2O$ (99%), $FeCl_2 \cdot 4H_2O$ (99%) were obtained from Aladdin (Shanghai, China). Water used throughout the work was produced by a Milli-Q ultrapure water system (Millipore, Bedford, Massachusetts, USA).

Instrumental

The magnetite nanoparticles were characterized by transmission electron microscopy (TEM), Fourier-transform infrared (FT-IR) spectroscopy, scanning electron microscope (SEM), and vibration sample magnetometer (VSM). TEM micrographs were obtained by the JEM2100F system (JEOL, Japan). SEM microstructure of nanoparticles was recorded by the S4800 system (Hitachi, Japan). The FT-IR spectra were recorded using KBr pellets on Nicolet iS50 spectrophotometer (Thermo Fisher Scientific, Waltham, Massachusetts, USA). The magnetic properties of nanoparticles were investigated by a VSM7407 (Lakeshore, Louisiana, USA).

High-Performance Liquid Chromatography Analysis

Chromatographic separation was performed on an analytical symmetry C18 column (250 × 4.6 mm i.d., 5 μm, Waters, Milford, Massachusetts, USA). The isocratic mobile phase consisted of water-methanol (15:85, v/v) with a flow rate of 1.0 ml/min was prepared for celecoxib analysis at 25°C and the chromatograms were acquired at 254 nm.

UPLC-Q-Exactive Orbitrap-MS/MS

The UPLC-MS/MS analysis of the eluent was performed on an analytical Shim-pack XR-ODS II (75 × 3.0 mm i.d., 1.7 μm, Shimadzu, Kyoto). The UPLC system mainly consisted of an Ultimate 3000 series ultra-high-performance liquid chromatography (Thermo Fisher Scientific, San Jose, USA) equipped with an online degasser, a quaternary pump, an

Time (min)	Flow rate (ml/min)	A (%)	B (%)
0–2	0.3	95–85	5–15
2–3	0.3	85–75	15–25
3–7	0.3	75–55	25–45
7–9	0.3	55–40	45–60
9–10	0.3	40–25	60–75
10.01–12	0.3	95	5

autosampler, and a column temperature compartment; it was connected to a Q-Exactive Orbitrap tandem mass spectrometer (Thermo Fisher Scientific, San Jose, USA) *via* an electrospray ionization interface (ESI). The mobile phase consisted of C (0.4% acetic acid in water) and D (acetonitrile) at 30°C, and the elution gradient as shown in **Table 1**. All the mobile phases were prepared daily.

Mass spectra were acquired in both the positive and negative ion mode through full MS and higher-energy collisional dissociation data-dependent MS/MS analysis. Full-scan high-resolution accurate-mass data acquisition captures all the sample data, enabling identification of untargeted compounds and retrospective data analysis without rerunning the samples.

Ion source parameters were shown as follows: spray voltage −3.0 kV (negative polarity) and 3.3 kV (positive polarity), sheath gas 35 arbitrary units, auxiliary gas 10 arbitrary units, capillary temperature 350°C, S-lens RF level 55, auxiliary gas heater temperature 350°C. Automatic gain control was set at 1e6, and the maximum injection time at 50 ms, and the isolation window at 2.0 *m/z*. The collision energy was varied in the range of 20–40 eV and scan range *m/z* 60–900 to obtain representative product ion spectra. The mass tolerance window was set to 5 ppm for the two analysis modes (2002/657/EC). Data analysis and processing have been performed using the Xcalibur 4.1 software (Thermo Scientific, USA).

Preparation of GO@Fe$_3$O$_4$@SiO$_2$-COX-2 Nanoparticles

Based on the previous report, some modifications were made to coat COX-2 on the GO layer (19).

The magnetic GO@Fe$_3$O$_4$ (MGO) nanoparticles were prepared by the chemical coprecipitation of Fe^{3+} and Fe^{2+}. At first, 0.50 g of GO was dispersed in 100 ml of distilled water and heated to 70°C. A total of 2.16 g of FeCl$_3$·6H$_2$O and 0.80 g of FeCl$_2$·4H$_2$O were dissolved in 40.0 ml of distilled water, and then added to the aforementioned dispersion suspension. After adjusting the pH to 10 with ammonia water (25%, w/v), the dispersion solution continued to be 70°C for 6 h. The whole process of the reaction was carried out under a stream of pure nitrogen. When the reaction finished, the suspension was filtered and washed three times with distilled water and ethanol, respectively.

Second, 6.3 ml of distilled water and 2.1 ml of TEOS were stirred for 3 min and sonicated for 1 min to obtain a milky solution. The milky solution was added to 49.5 ml of absolute ethanol including 0.50 g of magnetic GO@Fe$_3$O$_4$ nanoparticles. After stirring at 0°C for 10 min, 2.0 ml of glutaraldehyde was added dropwise to the dispersion solution. Then, the reaction lasted for 10 h. At last, separated by a magnet, GO@Fe$_3$O$_4$@SiO$_2$ (SMGO) nanoparticles were sequentially washed with 2% HNO$_3$, distilled water, and absolute ethanol in turn.

Finally, 0.10 g of SMGO nanoparticles were suspended in 50 ml ethanol-water solution (1:1, v/v), and adjusted the pH to 3–4 with 0.1 mol L^{-1} HCl. Followed by 1.0 ml APTES dropwise, the mixture was continued to be stirred for 5 h at 50°C. SMGO-NH$_2$ nanoparticles were separated by a permanent magnet and washed 4 times with ethanol. After being suspended in 5.0 ml of 5% glutaraldehyde solution for 1 h, the SMGO-NH$_2$ nanoparticles were retrieved by magnetic separation and washed with Tris-HCl buffer (100 mM, pH 8.0) three times to remove excess glutaraldehyde. Then shaken SMGO-NH$_2$ nanoparticles with 2.0 ml of tris-HCl buffer containing 50 units of COX-2 at 37°C for 2 h, the COX-2 functionalized magnetic microspheres (SMGO-COX-2) were synthesized.
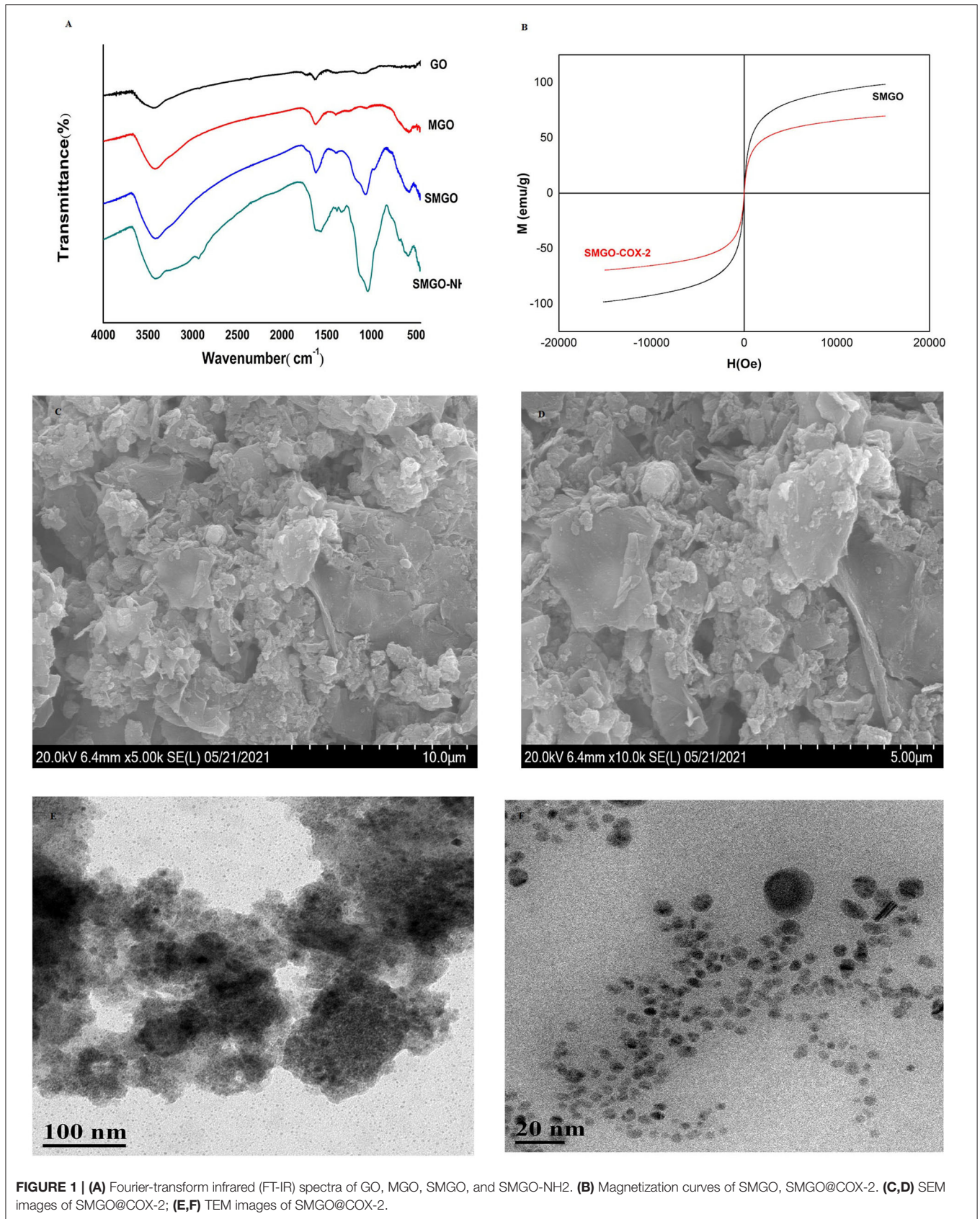
Magnetic Ligand Fishing in *Choerospondias axillaris*

A total of 5.0 g of *Choerospondias axillaris* powder was extracted with 500 ml of 75% (v/v) ethanol three times in parallel at 85°C for 1.5 h. After filtering on three layers of gauze of the diameter of 4.5 mm, the extraction solutions were combined, freeze-dried, and dissolved to 2 mg ml^{-1}. A total of 5 mg of COX-2 functional magnetic microspheres were suspended in 2 ml of extraction solution and incubated at 37°C for 30 min. Then, it was washed 3 times with 2 ml Tris-HCl buffer (pH 8.0) to remove non-specific binding ligands, and incubated with 1 ml of methanol for 1 h to dissociate the extracted ligand. After the nanoparticles were separated by a magnet, the elution solution had been filtered through a 0.22 μm membrane and then introduced into UPLC-Q-Exactive Orbitrap-MS/MS for analysis. Meanwhile, celecoxib was incubated with MGO, SMGO, and SMGO-inactive COX-2.

RESULTS AND DISCUSSION

Characterization of the Nanoparticles

Fourier-transform infrared spectroscopy analysis was used to record the surface functional groups and chemical bonds of synthetic materials. The infrared spectra of GO, MGO, SMGO, SMGO-NH$_2$ were shown in **Figure 1A**. The peak at 541 cm^{-1} was due to the tensile vibration of Fe-O-Fe. The strong absorption band at 1,066 cm^{-1} was attributable to the symmetric and asymmetric vibrations of Si-O-Si, indicating that GO was covered by Fe$_3$O$_4$ and SiO$_2$. The absorption at 1,300 cm^{-1} was attributed to the stretching vibration of C-N, indicating that SMGO was modified with the amino groups. Therefore, the results of FTIR analysis confirmed the formation of SMGO-NH$_2$ nanoparticles. The magnetic properties of the material were studied by VSM at room temperature. According to the curve in **Figure 1B**, the saturation magnetization of SMGO and SMGO-COX-2 was 98.42 and 69.60 emu·g^{-1}, respectively, which were enough to separate nanomaterials from the sample solution under an external magnetic field. Compared with SMGO, the

FIGURE 1 | (A) Fourier-transform infrared (FT-IR) spectra of GO, MGO, SMGO, and SMGO-NH2. **(B)** Magnetization curves of SMGO, SMGO@COX-2. **(C,D)** SEM images of SMGO@COX-2; **(E,F)** TEM images of SMGO@COX-2.

magnetization of SMGO-COX-2 was reduced by 28.82 emu·g^{-1}, which was attributed to the enzyme grafted on the surface of SiO$_2$. The morphology study of SMGO@COX-2 nanocomposite was shown in **Figures 1C,D**. Previous studies showed that GO was a single flake layer (19). After combining Fe$_3$O$_4$ particles, the surface becomes rough with spherical or elliptical substances. After coating SiO$_2$, the agglomeration phenomenon was reduced. After being connected to COX-2, the flake layer of GO was almost invisible, and the gaps created by the prevention of agglomeration of SiO$_2$ were also filled, and the entire surface became rougher and fuller. The structural morphology of SMGO@COX-2 nanocomposite was shown in **Figures 1E,F**. The black dots (SMGO@COX-2) on the cross-section were evenly anchored on the surface of the nanomaterial, and the shell-like layered structure could be seen inside the material.

Assay Verification

It is well known that compared with COX-1, celecoxib exhibits an extremely high-selective inhibitory effect on COX-2. The HPLC analysis were shown in **Figure 2**. When the COX-2 was bound to the surface of SMGO, the peak area of celecoxib in the elution solution increased significantly. Meanwhile, as shown in **Supplementary Figure S1**, when the inactive COX-2 was bound to the surface of SMGO, the peak area of celecoxib in the elution solution could be ignored. And extracted with MGO and SMGO, the celecoxib in the elution solution was rarely detected. Therefore, the results demonstrated the specificity of this magnetic ligand fishing for the screening of COX-2 ligands.

The stable activity of the immobilized enzyme COX-2 was a key prerequisite for capturing the same number of ligands during a series of binding-dissociation cycles. Therefore, the repeatability of SMGO@COX-2 was evaluated by specifically

capturing celecoxib. To avoid the loss of SMGO@COX-2 nanoparticles during the cycles, it was necessary to expose them to a magnetic field for 1 min. After 5 consecutive association-dissociation cycles, as shown in **Supplementary Figure S2**, the binding efficiency was still as high as 90% of the first cycle by calculating the peak area of celecoxib in the elution solution. The results showed a stable combination of SMGO and COX-2 and a high COX-2 ligand-binding capacity. After 5 days of storage at 4°C, as shown in **Supplementary Figure S3**, there was no significant loss on the celecoxib binding efficiency (RSD < 8%, $n = 5$), and three batches of SMGO@COX-2 showed similar binding efficiency (RSD < 10%).

Identification of COX-2 Inhibitors by UPLC-Q-Exactive Orbitrap-MS/MS

According to the retention time of each component, mass spectrum information, and related references, 21 COX-2 ligands were preliminarily determined in the eluted solution using magnetic ligand fishing technique as listed in **Table 2** and **Figures 3**, **4**. Both negative and positive ions were applied in the UPLC-Q-Exactive Orbitrap-MS/MS system to analyze the ligands of COX-2 separated from *Choerospondias axillaris*. The results in **Figure 3** showed that the eluted solution had better resolution of the references and more observable fragment ions in negative ion mode, which mainly attributed to the large amounts of phenolic acids and flavonoids.

Identification of Flavonoids

A total of 8 flavonoids have been identified in the elution solution of *Choerospondias axillaris*, accounting for more than 38%. In the negative mode ESI-MS spectra, the [M-H]$^-$ ion was observed for all the compounds. In the negative mode ESI-MS^2 spectra,
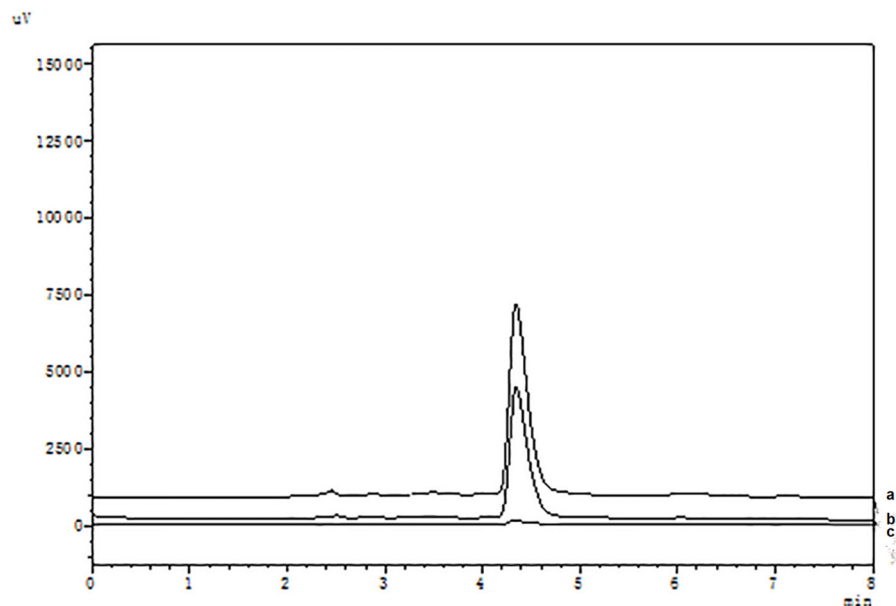
FIGURE 2 | High-performance liquid chromatography (HPLC) chromatograms of celecoxib (a) and ligand fishing assay eluent by SMGO-COX-2 (b), and SMGO (c).

TABLE 2 | Identification of elution solution by UPLC-Q-Exactive Orbitrap-MS/MS.

No.	Compounds	Chemical formula	R_t (min)	Ion mode	Observe mass (Da)	Error (ppm)	MS/MS	Confidential levels
1	Hydroquinone	$C_6H_6O_2$	5.03	−	109.02915	−3.325	81.03429[M-CO-H]$^-$	2
2	Succinic acid	$C_4H_6O_4$	0.43	−	117.01905	−2.409	73.02924[M-CO$_2$-H]$^-$	2
3	Protocatechualdehyde	$C_7H_6O_3$	4.69	−	137.02397	−3.265	93.03431[M-CO$_2$-H]$^-$	2
4	Protocatechuic acid	$C_7H_6O_4$	3.99	−	153.01891	−2.758	109.02916[M-CO$_2$-H]$^-$	2
							81.03448[M-CO$_2$-CO-H]$^-$	
5	Isovanillin	$C_8H_8O_3$	0.18	+	153.05443	−1.246	/	2
			3.80	−	151.03976	−2.035	136.01616[M-CH$_3$-H]$^-$	
							108.02154[M-CH$_3$-CO-H]$^-$	
6	Vanillic acid	$C_8H_8O_4$	5.02	−	167.03418	−4.801	152.01100[M-CH$_3$-H]$^-$	1
							108.02141[M-CH$_3$-CO$_2$-H]$^-$	
7	Gallic acid	$C_7H_6O_5$	1.2	−	169.01341	−4.95	125.02403[M-CO$_2$-H]$^-$	2
8	Caffeic acid	$C_9H_8O_4$	7.77	−	179.03459	−2.19	135.04480[M-CO$_2$-H]$^-$	1
9	Syringaldehyde	$C_9H_{10}O_4$	4.63	−	181.05003	−3.325	166.02614[M-CH$_3$-H]$^-$	2
							151.00313[M-2CH$_3$-H]$^-$	
10	Quinic acid	$C_7H_{12}O_6$	1.05	−	191.05539	−3.776	173.04510[M-H$_2$O-H]$^-$	2
11	Citric acid	$C_6H_8O_7$	6.03	−	191.01825	−7.726	111.00851[M-2H$_2$O-CO$_2$-H]$^-$	1
							87.00853[M-2CO$_2$-OH]$^-$	
12	Pantothenic acid	$C_9H_{17}NO_5$	3.39	+	220.11786	−0.405	202.10732[M-H$_2$O+H]$^+$	2
							124.07572[M-C$_2$H$_8$O$_4$+H]$^+$	
13	Palmitic acid	$C_{16}H_{32}O_2$	11.04	−	255.23247	−1.874	/	3
14	Pinocembrin	$C_{15}H_{12}O_4$	10.72	−	255.06573	−2.615	213.05482[M-C$_2$H$_2$O-H]$^-$	2
							151.00323[M-C$_8$H$_8$-H]$^-$	
15	Naringenin	$C_{15}H_{12}O_5$	8.56	−	271.06122	0.086	177.01860[M-C$_6$H$_7$O-H]$^-$	2
							151.00316[M-C$_6$H$_7$O-2CH$_3$-H]$^-$	
16	Kaempferol	$C_{15}H_{10}O_6$	7.57	−	285.04062	0.557	257.04523[M-CO-H]$^-$	2
17	Catechin	$C_{15}H_{14}O_6$	4.56	−	289.07175	0.039	245.08098[M-CO$_2$-H]$^-$	1
							203.07045[M-C$_4$H$_6$O$_2$-H]$^-$	
18	Ellagic acid	$C_{14}H_6O_8$	5.45	−	300.99771	−4.254	283.99567[M-H$_2$O-H]$^-$	1
							273.04050[M-CO-H]$^-$	
							229.04938[M-CO-CO$_2$-H]$^-$	
19	Quercetin	$C_{15}H_{10}O_7$	7.65	−	301.03439	−3.275	151.00316[M-C$_7$H$_6$O$_2$-CO-H]$^-$	1
							178.99800[M-C$_7$H$_6$O$_2$-H]$^-$	
							107.01353[M-C$_8$H$_6$O$_3$-CO$_2$-H]$^-$	
							121.02917[M-C$_8$H$_4$O$_5$-H]$^-$	
20	Taxifolin	$C_{15}H_{12}O_7$	6.05	−	303.04874	−7.543	285.04025[M-H$_2$O-H]$^-$	1
							125.02387[M-C$_9$H$_6$O$_4$-H]$^-$	
21	Rutin	$C_{27}H_{30}O_{16}$	4.96	−	609.14532	−1.293	300.02667[M-C$_{12}$H$_{20}$O$_9$-H]$^-$	1
							301.03378[M-C$_{12}$H$_{21}$O$_9$-H]$^-$	
							271.02411[M-C$_{12}$H$_{20}$O$_9$-H$_2$O-H]$^-$	
							255.02911[M-C$_{12}$H$_{22}$O$_{11}$-H]$^-$	

Confidential level 1: Compounds that matched to reference standard.
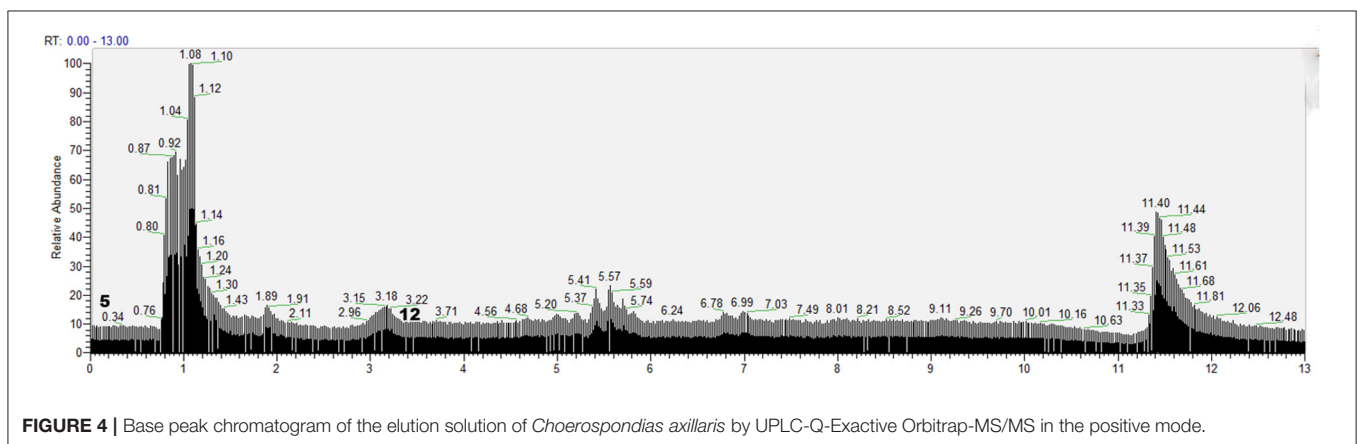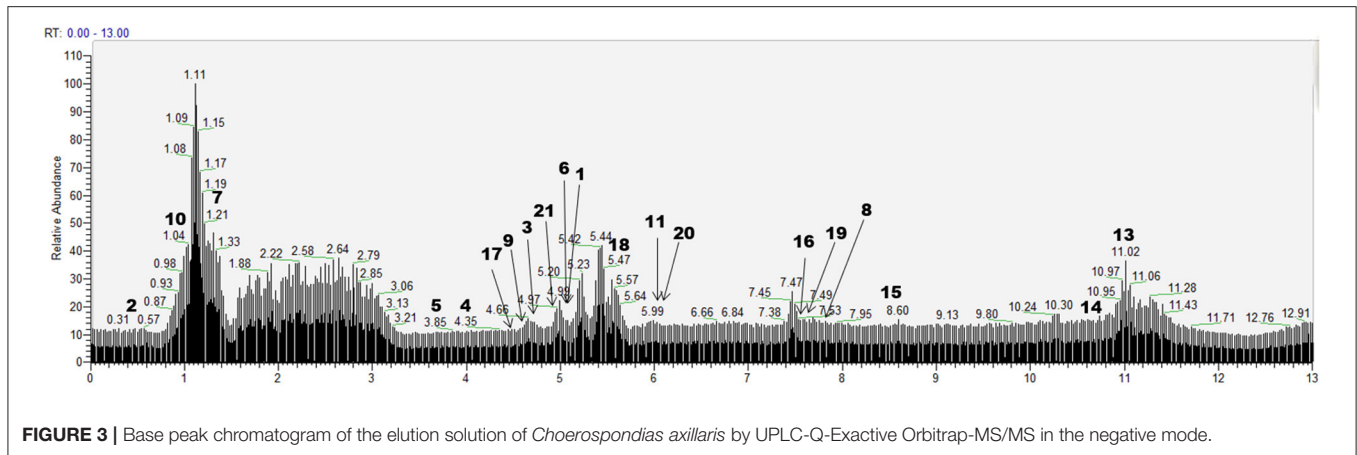*Confidential level 2: Compounds that matched to robust spectral or literatures.*
Confidential level 3: Compounds that classified.

the [M-A-H]$^-$ ion was observed for 6 compounds, such as compounds 14, 15, 16, 19, 20, and 21 (A represents various groups with more than 6 carbon atoms). The [M-CH$_3$-H]$^-$ ion was observed for 2 compounds, such as compounds 9 and 15. The [M-H$_2$O-H]$^-$ ion was observed for 2 compounds, such as compounds 20 and 21. The [M-CO-H]$^-$ ion was observed for 2 compounds, such as compounds 16 and 19. The [M-CO$_2$-H]$^-$ ion was observed for 2 compounds, compounds 17 and 19. From

this result, it can be seen that [M-H]$^-$ is the most fragmented ions, followed by [M-A-H]$^-$.

Identification of Phenolic Acids

A total of 6 phenolic acids have been identified in the elution solution of *Choerospondias axillaris*, accounting for more than 28%. In the negative mode ESI-MS spectra, the [M-H]$^-$ ion was observed for all the compounds. In the negative mode

FIGURE 3 | Base peak chromatogram of the elution solution of *Choerospondias axillaris* by UPLC-Q-Exactive Orbitrap-MS/MS in the negative mode.

FIGURE 4 | Base peak chromatogram of the elution solution of *Choerospondias axillaris* by UPLC-Q-Exactive Orbitrap-MS/MS in the positive mode.

ESI-MS^2 spectra, the $[M-CO_2-H]^-$ ion was observed for all the compounds. The $[M-CH_3-H]^-$ ion was observed for 1 compound, compounds 6. The $[M-H_2O-H]^-$ ion was observed for 1 compound, compounds 11. The $[M-CO-H]^-$ ion was observed for 1 compound, compounds 4. From this result, it can be seen that $[M-H]^-$ and $[M-CO_2-H]^-$ are the most fragmented ions in phenolic acids.

Identification of Other Compounds

A total of 6 other compounds including 2 aromatic aldehydes, 2 organic acids, and 2 phenols, have been identified in the elution solution of *Choerospondias axillaris*, accounting for more than 28%. In the negative mode ESI-MS spectra, the $[M-H]^-$ ion was observed for all the compounds. In the negative mode ESI-MS^2 spectra, the $[M-CO-H]^-$ ion was observed for 2 phenols and 1 aromatic aldehyde, compounds 1, 5, and 18. The $[M-CO_2-H]^-$ ion was observed for 1 phenol and 1 aromatic aldehyde, compounds 3 and 18. The $[M-H_2O-H]^-$ ion was observed for 1 organic acid and 1 aromatic aldehyde, compounds 10 and 18. And in the positive mode ESI-MS spectra, the $[M+H]^-$ ion was observed for all the compounds. In the positive mode ESI-MS spectra, the $[M-H_2O+H]^-$ ion was observed for 1 compound, compounds 12. From this result, it can be seen that $[M-H]^-$ and $[M-CO-H]^-$ are the most fragmented ions in other compounds.

Evaluate of COX-2 Inhibitors in *Choerospondias axillaris*

Consistent with our results, 21 bioactive compounds were reported to participate in the COX-2 inhibitory pathway in different forms. It is well known that LPS-induced reactive oxygen species production leads to COX-2 induction, and compounds 1, 3, 9, 15, 16, 19, and 20 were found to effectively inhibit the production of LPS-induced COX-2 metabolites (20–23). It has been reported that compound 8 suppressed UVB-induced COX-2 expression by blocking Fyn kinase activity (24). Meanwhile, compounds 4, 6, 13, and 14 suppressed the NF-κB signaling pathways to limit the expression of COX-2 (25–28). Differently, compounds 7, 10, 17, 18, and 21 were proven to reduce COX-2 levels by reducing nitric oxide overproduction from inducible nitric oxide synthase (29–31). Considering the aforementioned facts, we can still conclude that, the compounds analyzed by UPLC-Q-Exactive Orbitrap MS/MS were consistent.

CONCLUSION

Choerospondias axillaris has complex components and diverse structures, which has the effect on multiple targets. Network pharmacology showed that their anticoronary heart disease action pathway was mainly through anti-inflammation,

which provided theoretical support to choose the target of COX-2. And this study aimed to establish a fast and simple method to target and screen out the active compounds that interacted with COX-2 from *Choerospondias axillaris*, and it was the first time that synthesized COX-2 magnetic microspheres were applied to extract COX-2 inhibitors. Meanwhile, the COX-2 functionalized magnetic microspheres in this method had excellent specificity, good precision, low cost, and high-throughput screening efficiency. Therefore, the method could be used to immobilize macromolecular targets and provide convenient conditions for screening many specific biologically active compounds from complex natural products.

DATA AVAILABILITY STATEMENT

The original contributions presented in the study are included in the article/**Supplementary Material**, further inquiries can be directed to the corresponding author/s.

AUTHOR CONTRIBUTIONS

MC helped in writing the original draft, data curation, and formal analysis. HW was involved in methodology, project administration, and validation. ZY helped with the investigation and resources. LC worked with software and visualization. XG was involved in the reviewing and editing and funding acquisition. KQ helped with supervision and conceptualization. All authors contributed to the article and approved the submitted version.

FUNDING

SUPPLEMENTARY MATERIAL

The Supplementary Material for this article can be found online at: https://www.frontiersin.org/articles/10.3389/fnut.2021.794193/full#supplementary-material

Supplementary Figure S1 | The HPLC chromatograms of celecoxib (a) and ligand fishing assay eluent by SMGO-COX-2 (b), MGO (c), SMGO-inactive COX-2 (d), and SMGO (e).

Supplementary Figure S2 | The HPLC chromatograms of celecoxib in five consecutive association-dissociation cycles of ligand fishing assay eluent by SMGO-COX-2.

Supplementary Figure S3 | The HPLC chromatograms of celecoxib in ligand fishing assay eluent by SMGO-COX-2 during five days of storage at 4°C.

REFERENCES

1. Zhou J, Mei SG. Research progress of Mongolian Medicine Guangzhao. *Strait Pharm J.* (2017) 29:1–5. doi: 10.3969/j.issn.1006-3765.2017.06.001

2. Li L, Li J, Yi J, Liu H, Lei H. Dose–effect of irbesartan on cyclooxygenase-2 and matrix metalloproteinase-9 expression in rabbit atherosclerosis. *J Cardiovasc Pharmacol.* (2018) 71:82. doi: 10.1097/FJC.0000000000000544

3. Dang Z, Su S, Jin G, Nan X, Ma L, Li Z, et al. Tsantan Sumtang attenuated chronic hypoxia-induced right ventricular structure remodeling and fibrosis by equilibrating local ACE-AngII-AT1R/ACE2-Ang1-7-Mas axis in rat. *J Ethnopharmacol.* (2019) 250:112470. doi: 10.1016/j.jep.2019.112470

4. Morrison A, Li J. PPAR-γ and AMPK-Advantageous targets for myocardial ischemia/reperfusion therapy. *Biochem Pharmacol.* (2011) 82:195–200. doi: 10.1016/j.bcp.2011.04.004

5. Gao X, Mu J, Guan S, Li Q, Du Y, Zhang H, et al. Simultaneous determination of phenolic acids and diterpenoids and their comparative pharmacokinetic study in normal and acute blood stasis rats by UFLC–MS/MS after oral administration of Guan-Xin-Shu-Tong capsules. *J Chromatogr B.* (2018) 1072:221–8. doi: 10.1016/j.jchromb.2017.11.017

6. Smith JP, Haddad EV, Downey JD, Breyer RM, Boutaud O. PGE2 decreases reactivity of human platelets by activating EP2 and EP4. *Thromb Res.* (2010) 126:23–9. doi: 10.1016/j.thromres.2010.04.003

7. Sanak M, Plutecka H, Szczeklik W, Piwowarska W, Rostoff P, Szczeklik A. Functional promoter polymorphism of cyclooxygenase-2 modulates the inflammatory response in stable coronary heart disease. *Polskie Arch Med Wewntrznej.* (2010) 120:82–8 doi: 10.1371/journal.pmed.1000222

8. Liu J, Wang S, Tan W, Lv B, Dai Y, Wang Y. Dual-screening of anti-inflammatory and antioxidant active ingredients of shenxiang suhe pill and its potential multi-target therapy for coronary heart disease. *Biomed Pharmacother.* (2020) 129:110283. doi: 10.1016/j.biopha.2020.110283

9. Bagdas D, Muldoon PP, AlSharari S, Carroll FI, Negus SS, Damaj MI. Expression and pharmacological modulation of visceral pain-induced conditioned place aversion in mice. *Neuropharmacology.* (2016) 102:236–43. doi: 10.1016/j.neuropharm.2015.11.024

10. Mosaddeque F, Mizukami S, Teklemichael AA, Mizuta S, Tanaka Y, Taniguchi M, et al. Prediction Model for Antimalarial Activities of Hemozoin Inhibitors by Using Physicochemical Properties. Antimicrob Agents Chemother.(2018) 62:e02424-17. doi: 10.1128/AAC.02424-17

11. Geromichalos GD, Alifieris CE, Geromichalou EG, Trafalis DT. Overview on the current status on virtual high-throughput screening and combinatorial chemistry approaches in multi-target anticancer drug discovery; Part II. *J Balkan Union Oncol.* (2016) 21:1337–58

12. Cerqueira NM, Gesto D, Oliveira EF, Santos-Martins D, Brás NF, Sousa SF, et al. Receptor-based virtual screening protocol for drug discovery. *Arch Biochem Biophys.* (2015) 582:56–67. doi: 10.1016/j.abb.2015.05.011

13. Zaouak A, Noomen A, Jelassi H. Gamma radiation induced degradation of the phenoxy acid herbicide diclofop-methyl in aqueous solutions. *Appl Rad Isotopes.* (2020) 156:108939. doi: 10.1016/j.apradiso.2019.108939

14. Zhang Y, Nie M, Shi S, You Q, Guo J, Liu L. Integration of magnetic solid phase fishing and off-line two-dimensional high-performance liquid chromatography-diode array detector-mass spectrometry for screening and identification of human serum albumin binders from Radix Astragali. *Food Chem.* (2014) 146:56–64. doi: 10.1016/j.foodchem.2013.09.030

15. Li Y, Chen Y, Xiao C, Chen D, Xiao Y, Mei Z. Rapid screening and identification of alpha-amylase inhibitors from Garcinia xanthochymus using enzyme-immobilized magnetic nanoparticles coupled with HPLC and MS. *J Chromatogr B Anal Technol Biomed Life Sci.* (2014) 960:166–73. doi: 10.1016/j.jchromb.2014.04.041

16. Tao Y, Zhang Y, Cheng Y, Wang Y. Rapid screening and identification of α-glucosidase inhibitors from mulberry leaves using enzyme-immobilized magnetic beads coupled with HPLC/MS and NMR. *Biomed Chromatogr.* (2013) 27:148–55. doi: 10.1002/bmc.2761

17. Zhang Y, Shi S, Chen X, Peng M. Functionalized magnetic nanoparticles coupled with mass spectrometry for screening and identification of cyclooxygenase-1 inhibitors from natural products. *J Chromatogr B Anal Technol Biomed Life Sci.* (2014) 960:126–32. doi: 10.1016/j.jchromb.2014.04.032

18. Vanzolini KL, Ainsworth S, Bruyneel B, Herzig V, Seraus MG, Somsen GW, et al. Rapid ligand fishing for identification of acetylcholinesterase-binding peptides in snake venom reveals new properties of dendrotoxins. *Toxicon.* (2018) 152:1–8. doi: 10.1016/j.toxicon.2018.06.080

19. Suo L, Zhao J, Dong X, Gao X, Li X, Xu J, Zhao L. Functionalization of a SiO2-coated magnetic graphene oxide composite with polyaniline–polypyrrole for magnetic solid phase extraction of ultra-trace Cr(iii) and Pb(ii) in water and food samples using a Box–Behnken design. *New J Chem.* (2019) 43:12126–36. doi: 10.1039/c9nj02038a

20. Stanikunaite R, Khan SI, Trappe JM, Ross SA. Cyclooxygenase-2 inhibitory and antioxidant compounds from the truffle *Elaphomyces granulatus*. *Phytother Res.* (2009) 23:575–8. doi: 10.1002/ptr.2698

21. Hämäläinen M, Nieminen R, Asmawi MZ, Vuorela P, Vapaatalo H, Moilanen E. Effects of flavonoids on prostaglandin E2 production and on COX-2 and mPGES-1 expressions in activated macrophages. *Planta Med.* (2011) 77:1504–11. doi: 10.1055/s-0030-1270762

22. Chang ZQ, Gebru E, Lee SP, Rhee MH, Kim JC, Cheng H, et al. In vitro antioxidant and anti-inflammatory activities of protocatechualdehyde isolated from *Phellinus gilvus*. *J Nutr Sci Vitaminol.* (2011) 57:118–22. doi: 10.3177/jnsv.57.118

23. Ajayi AM, Badaki VB, Ariyo OO, Ben-Azu B, Asejeje FO, Adedapo AD. Chrysophyllum albidum fruit peel attenuates nociceptive pain and inflammatory response in rodents by inhibition of pro-inflammatory cytokines and COX-2 expression through suppression of NF-κB activation. *Nutr Res.* (2020) 77:73–84. doi: 10.1016/j.nutres.2020.03.004

24. Kang NJ, Lee KW, Shin BJ, Jung SK, Hwang MK, Bode AM, Dong Z. Caffeic acid, a phenolic phytochemical in coffee, directly inhibits Fyn kinase activity and UVB-induced COX-2 expression. *Carcinogenesis.* (2008) 30: 321–330. doi: 10.1093/carcin/bgn282

25. Giri SS, Sen SS, Sukumaran V, Park SC. Pinocembrin attenuates lipopolysaccharide-induced inflammatory responses in Labeo rohita macrophages *via* the suppression of the NF-κB signalling pathway. *Fish Shellfish Immunol.* (2016) 56:459–66. doi: 10.1016/j.fsi.2016.07.038

26. de Souza CO, Valenzuela CA, Baker EJ, Miles EA, Rosa Neto JC, Calder PC. Palmitoleic acid has stronger anti-inflammatory potential in human endothelial cells compared to oleic and palmitic acids. *Mol Nutr Food Res.* (2018) 62:e1800322. doi: 10.1002/mnfr.201800322

27. Huang X, Xi Y, Mao Z, Chu X, Zhang R, Ma X, et al. Vanillic acid attenuates cartilage degeneration by regulating the MAPK and PI3K/AKT/NF-κB pathways. *Eur J Pharmacol.* (2019) 859:172481. doi: 10.1016/j.ejphar.2019.172481

28. Adeyanju AA, Asejeje FO, Molehin OR, Owoeye O, Olatoye EO, Ekpo EN. Protective role of protocatechuic acid in carbon tetrachloride-induced oxidative stress *via* modulation of proinflammatory cytokines levels in brain and liver of Wistar rats. *J Basic Clin Physiol Pharmacol.* (2021) 3:20200202. doi: 10.1515/jbcpp-2020-0202

29. BenSaad LA, Kim KH, Quah CC, Kim WR, Shahimi M. Anti-inflammatory potential of ellagic acid, gallic acid and punicalagin A and B isolated from *Punica granatum*. *BMC Complement Altern Med.* (2017) 17:47. doi: 10.1186/s12906-017-1555-0

30. Lee KP, Choi NH, Kim HS, Ahn S, Park IS, Lee DW. Anti-neuroinflammatory effects of ethanolic extract of black chokeberry (*Aronia melanocapa* L.) in lipopolysaccharide-stimulated BV2 cells and ICR mice. *Nutr Res Pract.* (2018) 12:13–19. doi: 10.4162/nrp.2018.12.1.13

31. Amparo TR, Seibert JB, Mathias FA, Vieira JF, Soares RD, Freitas KM, et al. Anti-inflammatory activity of *Protium spruceanum* (Benth.) Engler is associated to immunomodulation and enzymes inhibition. *J Ethnopharmacol.* (2019) 241:112024. doi: 10.1016/j.jep.2019.112024